Optical properties of aluminum-doped zinc oxide films deposited by direct-current pulse magnetron reactive sputtering*

Gao Xiao-Yong(郜小勇)†, Chen Chao(陈 超), and Zhang Sa(张 飒)

School of Physics and Engineering, Zhengzhou University, Zhengzhou 450052, *China*

(Received 7 June 2013; revised manuscript received 4 September 2013; published online 14 January 2014)

A series of ⟨103⟩-oriented aluminum-doped zinc oxide (AZO) films were deposited on glass substrates via direct-current pulse magnetron reactive sputtering at different O_2-to-Ar gas flow ratios (GFRs). The optical properties of the films were characterized using the fitted optical constants in the general oscillator model (which contains two Psemi-Tri oscillators) through the use of measured ellipsometric parameters. The refractive index dispersion data below the interband absorption edge were analyzed using a single-oscillator model. The fitted optical energy gap obtained using the single-oscillator model clearly shows a blue shift, followed by a red shift, as the GFR increases from 0.9/18 to 2.1/18. This shift can be attributed to the change in the free electron concentration of the film, which is closely related to the film stress. In addition, the fitted β value indicates that the AZO film falls under the ionic class. The photoluminescence spectrum indicates a photoluminescence mechanism of the direct and wide energy gap semiconductor.

Keywords: AZO film, spectroscopic ellipsometry, single-oscillator model

PACS: 07.60.Fs, 78.20.–e, 77.55.hf **DOI:** 10.1088/1674-1056/23/3/030701

1. Introduction

Aluminum-doped zinc oxide (AZO) is a wide and direct energy gap semiconductor whose energy gap can be adjusted between 2.8 and 4.2 eV.[1] The large exciton binding energy (60 meV), prominent piezoelectricity, and stability in hydrogen plasma environment[2] make AZO films have a potential application in photovoltaic and piezoelectric devices, as well as in gas and piezo sensors.[3–5] As previously reported, a variety of physical and chemical methods can be used to synthesize AZO thin films, including magnetron sputtering, evaporation, chemical vapor deposition, sol–gel technique, and pulsed laser deposition. Of these, magnetron sputtering produces uniform and large-sized films with a high deposition rate. Kluth *et al.*[6] adopted different sputtering techniques (direct-current (DC), radio, and middle-frequency) to prepare AZO films using a ceramic target (ZnO/Al_2O_3) and an alloy target (Zn:Al). The results show that the electricity and structure of AZO films are closely related to pressure and the substrate temperature. Zhang *et al.*[7] prepared polycrystalline ZnO films via radio frequency (RF) sputtering and studied their photoresponse and structural change. Kim *et al.*[8] obtained *c*-axis oriented AZO films of hexagonal crystalline structure with a ceramic target (ZnO/Al_2O_3) via RF sputtering, with the lowest resistivity of 4.7×10^{-4} Ω·cm. Agura *et al.*[9] used a pulsed laser deposition method to obtain an AZO film with a resistivity of 8.54×10^{-5} Ω·cm by controlling the laser energy density. In addition, Gao *et al.*[10] reported that substrate temperature strongly affects the electrical and optical properties of AZO films deposited via direct-current pulse (DCP) magnetron reactive sputtering. Compared with DC and DCP sputtering, the high-power RF sputtering system costs higher and is harmful to human health because of its radiation injury, thus it is rarely applied in industry.

Spectroscopic ellipsometry (SE) is an effective method of measuring the dielectric constants based on the appropriate system model. However, the relationship between the dielectric constants and the structural and optical properties is difficult to establish via spectroscopic ellipsometry alone. In this article, the dielectric constants of an AZO film deposited via DCP sputtering at different O_2-to-Ar gas flow ratios (GFRs) were fitted in terms of the general oscillator model (a parameterized semiconductor oscillator model combined with two Psemi-Tri oscillators[11]) using the measured ellipsometric spectra to investigate the interband transitions. The refractive index dispersion data below the interband absorption edge of the film were analyzed using a single-oscillator model. The photoluminescence (PL) spectrum of the film was also obtained to verify the results of spectroscopic ellipsometry.

2. Experimental procedure

A series of AZO films were deposited on a glass substrate via DCP sputtering using GFR ranging from 0.9/18 to 2.1/18 at a substrate temperature of 250 °C. The DCP sputtering system used a 40-kHz DCP signal with an 80% voltage duty circle. A high-purity (> 99.99%) Zn–Al alloy plate (220 mm×80 mm×5 mm) with an Al content of 3.0 wt% was

*Project supported by the National Natural Science Foundation of China (Grant No. 60807001), the Foundation of Young Key Teachers from University of Henan Province, China (Grant No. 2011GGJS-008), the Foundation of Graduate Education Support of Zhengzhou University, China, and the Foundation of Graduate Innovation of Zhengzhou University, China (Grant No. 12L00104).

†Corresponding author. E-mail: xygao@zzu.edu.cn

© 2014 Chinese Physical Society and IOP Publishing Ltd

used as the sputtering target. The sputtering power was 125 W, the electrode distance was 35 mm, and the working pressure was maintained at 0.5 Pa. The glass substrate was first pretreated and then sequentially rinsed with acetone and alcohol in an ultrasonic bath for 15 min to remove grease and other soluble organics on the surface. The substrate was then placed in an ultrahigh vacuum chamber previously evacuated to a base pressure below 1.0×10^{-3} Pa and heated to 250 °C to obtain a clean substrate surface.

The film microstructure was measured using an X-ray diffractometer (XRD, Philips PANAlytical X'pert), and cold-field scanning electron microscope (JSM-6700F). A Cu K_α (λ = 0.1540598 nm) was used as the X-ray source, and the XRD spectra was measured with a grazing angle of 5°. The optical constants of the film were fitted in the general oscillator model using the measured SE spectra from a variable-angle spectroscopic ellipsometry (VASE, J. A. woollam Company). The refractive index dispersion data below the interband absorption edge were analyzed using a single-oscillator model. Additionally, the PL spectrum of the film was measured by a PL spectrum tester (FluoroMax-4 type) with a xenon lamp as irradiation source.

3. Results and discussion

3.1. Structural properties

The XRD patterns of the deposited AZO films in this work have been reported elsewhere.[12] The as-deposited AZO films are polycrystalline and preferentially oriented in the ⟨103⟩ direction rather than the usual ⟨002⟩ orientation reported.[13] The lattice constant c of the film is determined as $c = 2d_{(002)}$ based on the spacing of the (002) crystalline face. The peak position of the ZnO (002) diffraction peak clearly deviates slightly from the standard value of the ZnO (002) diffraction peak. This deviation is attributed to the film stress (σ), which can be expressed using the dual-axis stress model, as follows:[14]

$$\sigma = [2C_{13}^2 - C_{33}(C_{11}+C_{12})]\varepsilon/(2C_{13}), \quad (1)$$

$$\varepsilon = (d_{\text{film}} - d_{\text{ZnO}})/d_{\text{ZnO}}, \quad (2)$$

where ε is the film strain along the ⟨002⟩ orientation, d_{film} and d_{ZnO} are the d-spacing of the (002) plane of the AZO and pure ZnO films, respectively, C_{ij} is the elastic modulus of the bulk ZnO films,[15] and $C_{11} = 208.8$ GPa, $C_{12} = 119.7$ GPa, $C_{13} = 104.2$ GPa, and $C_{33} = 213.8$ GPa. Figure 1 shows the d-spacing of the (002) crystalline face and the film stress (σ) of the AZO films as a function of GFR. The compressive stress initially increases to the maximum value, and then gradually decreases as the GFR value increases. The transition from compressive to tensile stress occurs with GFR increasing. The change of the stress with the GFR value may be inherently related to that of the crystalline structure.

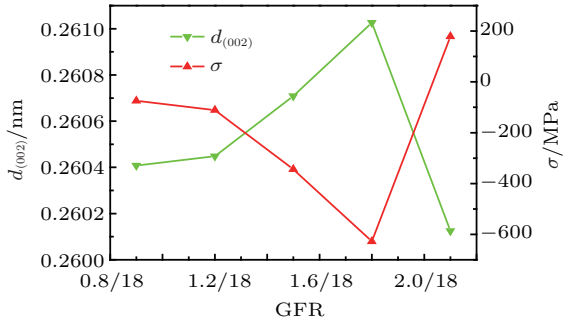


Fig. 1. (color online) d-spacing of the (002) crystalline face and the film stress of the AZO films as a function of GFR.

3.2. Optical properties

In the SE analysis, the modeling parameters of interest, i.e., the dielectric constants and layer thickness, are varied to achieve the best fit between the calculated and experimental SE parameters (Ψ and Δ). The film mass thickness (d_{f}) is defined as[16]

$$d_{\text{f}} = d_{\text{b}} + 0.5d_{\text{s}}, \quad (3)$$

where d_{b} and d_{s} are the thicknesses of the film and surface roughness layers, respectively. Table 1 shows the fitted d_{f} and the parameters used in the general oscillator model for the AZO films, with the mean-square error under 10. Here, E_{c} and B_{r} are oscillator center energy and broadening parameter, respectively, WL and WR denote endpoint positions relative to the center energy; AL and AR denote relative magnitude of the left and right control points compared to the amplitude (i.e., Amp). Figure 2 shows the measured and fitted Ψ and Δ of the AZO film deposited at GFR = 1.5/18. The fitted Ψ and Δ values are clearly in accordance with the measured values. The extracted refractive index n and extinctive coefficient k of the deposited AZO films at different GFR values are shown in Fig. 3. An evident abnormal dispersion occurs as the photon energy surpasses a threshold value of approximately 3.34 eV, whereas the extinctive coefficient sharply increases above the threshold value. This result indicates that an interband absorption occurs around the threshold value.

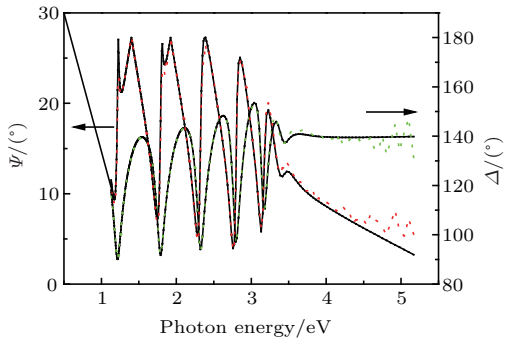


Fig. 2. (color online) Measured and fitted ellipsometric parameters Ψ and Δ of the AZO film deposited at the GFR = 1.5/18. Solid line denotes the measurement values.

Table 1. Fitted film mass thickness (d_f) and parameters used in the general oscillator model for the AZO films.

GFR	Osc. No.	Amp	E_c/eV	B_r/eV	WL/eV	WR/eV	AL	AR	d_f/nm
0.9/18	1	0.8852	3.565	0.1	0.44762	3.7895	0.08920	0.97877	698
	2	0.9165	13.608	0.1	11.299	25.269	0.43299	0.26872	
1.2/18	1	0.7174	3.4208	0.1	0.25903	2.1279	0.14202	0.999	685
	2	1.0368	9.5603	0.1	6.9593	30.668	0.41918	0.51622	
1.5/18	1	1.3031	3.6533	0.1	1.7299	8.164	0.00590	0.72566	632
	2	0.2361	13.223	0.1	71.226	3.7805	0.25721	0.52233	
1.8/18	1	1.3072	3.7067	0.1	1.9038	8.2263	0.001	0.71197	588
	2	0.3859	14.159	0.1	68.534	2.827	0.27154	0.3509	
2.1/18	1	0.9776	3.6118	0.1	1.5289	5.5144	0.001	0.80728	516
	2	0.8561	13.44	0.1	12.082	10.391	0.17699	0.56725	

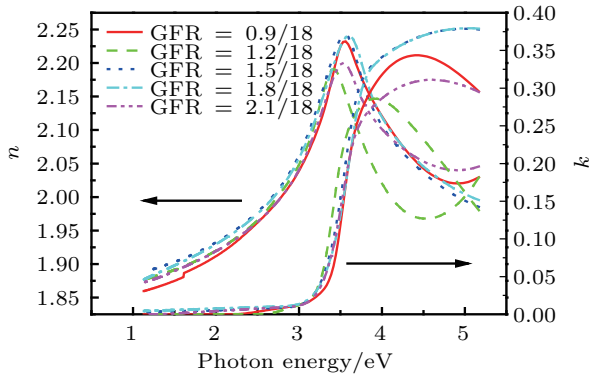


Fig. 3. (color online) Fitted refractive index and extinctive coefficient spectra of the deposited AZO films at different GFRs.

A single-oscillator model suggested by Wemple and DiDomenico was used to estimate the energy band structure of the AZO film and describe the hidden optical origin and mechanism by defining the dispersion-energy parameter E_d. For the single-oscillator model, the dispersion function in the visible region was formalized as[17]

$$n^2 - 1 = E_o E_d / (E_{o2} - E^2), \tag{4}$$

where n is the refractive index, E is the photon energy, and E_o and E_d are the single oscillator and dispersive energies, respectively, E_o and E_d are significantly correlated with the crystalline structure and the ionicity of ionic or covalent oxide materials. Figure 4 shows the plot of the refractive index factor $1/(n^2-1)$ versus E^2 for the deposited AZO films at different GFRs. The refractive index data were obtained from the SE fitting. The resulting straight line then yields values of E_o and E_d. For large groups of crystals containing a single anion species, E_d is empirically described as[17,18]

$$E_d = \beta N_c Z_a N_e, \tag{5}$$

where β always takes the ionic value of (0.26 ± 0.04) eV

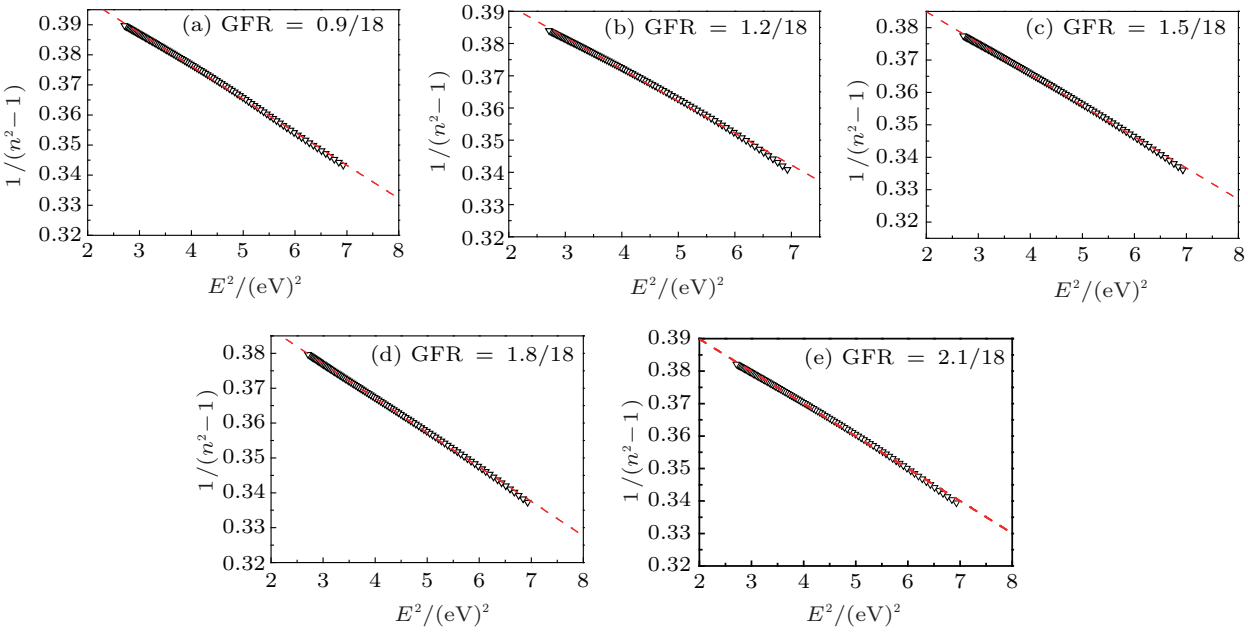


Fig. 4. (color online) Plot of refractive index factor $1/(n^2-1)$ versus $1/E^2$ for the AZO films deposited at GFR of (a) 0.9/18, (b) 1.2/18, (c) 1.5/18, (d) 1.8/18, and (e) 2.1/18.

for halides and most oxides; N_c is the coordination number of the cations nearest the anion; Z_a is the formal chemical valency of the anion; and N_e is the efficient number of valence electrons per anion (usually equal to 8). For ZnO (taking $N_e = 8$, $N_c = 4$, $Z_a = 2$), the calculated values of β with the increase of GFR value are 0.2297, 0.2445, 0.2502, 0.2466, 0.2444, which indicates that the AZO falls under the ionic class.

In terms of the single-oscillator model, the band gap E_a introduced by Hopfield[19] provides the link between the single-oscillator parameters (E_o, E_d) and the Phillips static-dielectric constant parameters (E_g, $\hbar\omega_p$), as follows:

$$E_o E_a = E_g^2, \tag{6}$$

$$E_a E_d = (\hbar\omega_p)^2, \tag{7}$$

where E_g and $\hbar\omega_p$ are the optical energy gap and plasma oscillator energies, respectively, and E_o obeys an empirical relationship ($E_o \approx 2E_g$[18,20]). The calculated E_g and $\hbar\omega_p$ (Fig. 5) show similar change tendencies as the GFR value increases. A blueshift in E_g initially occurs as the GFR increases to 1.5/18, followed by a redshift. To confirm the fitted E_g in terms of Eqs. (6) and (7), the PL spectrum of the AZO film deposited at GFR = 1.2/18 was obtained and is shown in Fig. 6. The excitation wavelength was 300 nm. The PL peak centered at approximately 3.147 eV almost coincides with the fitted direct interband transition value, indicating a direct-energy gap PL mechanism for the AZO film.

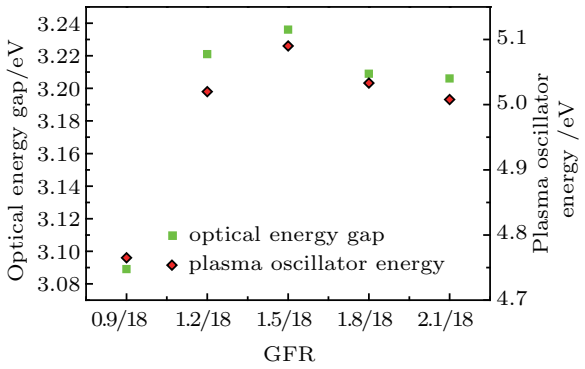


Fig. 5. (color online) Calculated optical energy gap E_g and plasma oscillator energy $\hbar\omega_p$ of the AZO films as a function of GFR.

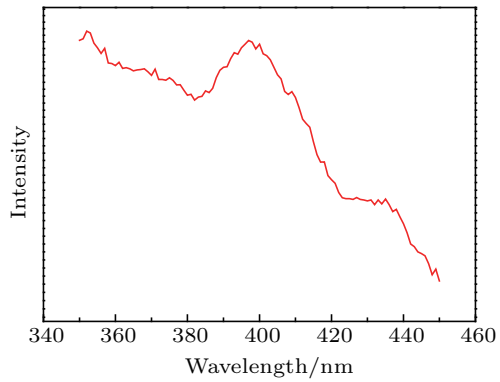


Fig. 6. (color online) Photoluminescence spectrum of the AZO film deposited at the GFR = 1.2/18.

The shift in the absorption edge of an n-type semiconductor is expressed in the following equation:[21]

$$\Delta E_{BM} = h^2(3\pi^2 N_e)^{2/3}/(2m_{ve}^* e), \tag{8}$$

where m_{ve}^* is the reduced effective mass, N_e is the free electron concentration, and e is the electronic charge. A slight blueshift in the absorption edge may be attributed to the increased free electron concentration, known as the Burstein Moss effect;[22] however, the mechanism for a slight redshift remains to be agreed on. Some researchers suggest that the redshift in E_g is associated with the relaxation of the compressive stress along the direction of the dislocation and grain,[23] whereas others argue that the defects around the surface may also contribute to the redshift in the optical band gap. According to our result, the change in E_g is similar to the transition from compressive to tensile stress as GFR increases, indicating that the shift in the absorption edge of the AZO films may be attributed to the transition of the film stress, and that the free electron concentration is closely related to the film stress. The GFR value affects the crystalline structure which affects the film stress and the free electron concentration. A modulated strain could be introduced to achieve a quantum confinement of the carriers.[23]

4. Conclusions

The AZO films deposited via DCP sputtering at different GFR values are ⟨103⟩ preferentially oriented. The optical constants of the AZO film were obtained by fitting the SE data in the general oscillator model. An evident abnormal dispersion occurs at a photon energy above 3.34 eV. Analysis of the refractive index dispersion relation using the single-oscillator model shows that the AZO film falls under the ionic class. A blueshift in E_g initially takes place as the GFR value increases to 1.5/18, followed by a redshift. The blueshift in the absorption edge is attributed to the increased free electron concentration, whereas the redshift is attributed to the transition of the film stress from compressive to tensile stress.

References

[1] Minemoto T, Negami T, Nishiwaki S, Takakura H and Hamakawa Y 2000 *Thin Solid Films* **372** 173
[2] Song D, Aberle A G and Xia J 2002 *Appl. Surf. Sci.* **195** 291
[3] Vanheusden K, Warren W L and Seager C H 1996 *J. Appl. Phys.* **79** 7983
[4] Chopra K L, Major S and Pandya D K 1983 *Thin Solid Films* **102** 1
[5] Granqvist C G 1990 *Thin Solid Films* **193–194** 730
[6] Kluth O, Schöpe G, Hüpkes J, Agashe C, Müller J and Rech B 2003 *Thin Solid Films* **442** 80
[7] Zhang D H and Brode D E 1995 *Acta Phys. Sin.* **44** 1321 (in Chinese)
[8] Kim K H, Park K C and Ma D Y 1997 *J. Appl. Phys.* **81** 7764
[9] Agura H, Suzuki A, Matsushita T, Aoki T and Okuda M 2003 *Thin Solid Films* **445** 263
[10] Gao X Y, Lin Q G, Feng H L, Liu Y F and Lu J X 2009 *Thin Solid Films* **517** 4684
[11] Woollam J A Co. Inc. 2011 *Complete EASE Software Manual* p. 338
[12] Chen C, Ji Y, Gao X Y, Zhao M K, Ma J M, Zhang Z Y and Lu J X 2012 *Acta Phys. Sin.* **61** 036104 (in Chinese)

[13] Chen X C, Zhou J P, Wang H Y, Xu P S and Pan G Q 2011 *Chin. Phys. B* **20** 096102
[14] Segmuller A and Murakami M 1988 *Analytical Techniques for Thin Films*, eds. by Tu K N and Rosenberg R (Boston: Academic Press) pp. 143–200
[15] Cebulla R, Wendt R and Ellmer K 1997 *J. Appl. Phys.* **83** 1087
[16] Ma J M, Liang Y, Gao X Y, Chen C, Zhao M K and Lu J X 2012 *Acta Phys. Sin.* **61** 056106 (in Chinese)
[17] Wemple S H and DiDomenico M J 1971 *Phys. Rev. B* **3** 1338
[18] Goldsmith S, ÇetinörgüE and Boxman R L 2009 *Thin Solid Films* **517** 5146
[19] Hopfield J J 1970 *Phys. Rev. B* **2** 973
[20] You Z Z and Hua G J 2009 *Vacuum* **83** 984
[21] Roth A P, Webb J B and Williams D F 1981 *Solid State Commun.* **39** 1269
[22] Burstein E 1954 *Phys. Rev.* **93** 632
[23] Tan I H, Lishan D, Mirin R, Jayaraman V, Yasuda T, Hu E L and Bowers J 1991 *Appl. Phys. Lett.* **59** 1875